Formation of Fabry-Perot resonances in double-barrier chaotic billiards

A. M. S. Macêdo

Departamento de Física, Laboratório de Física Teórica e Computacional, Universidade Federal de Pernambuco,
50670-901 Recife, PE, Brazil

Andre M. C. Souza

Universidade Federal de Sergipe, São Cristovão-SE, Brazil
(Received 11 November 2004; published 30 June 2005)

We study wave transport through a chaotic quantum billiard attached to two waveguides via barriers of arbitrary transparencies in the semiclassical limit of a large number of open scattering channels. We focus attention on the ergodic regime, which is described by using a random-matrix approach to chaotic resonance scattering together with an extended version of Nazarov's circuit theory. By varying the relative strength of the barriers' transparencies a reorganization of the relevant resonances in the energy interval where transport takes place leads to a full suppression of high transmission modes. We provide a detailed quantitative description of the process by means of both numerical and analytical evaluations of the average density of transmission eigenvalues. We show that the density of Fabry-Perot modes can be used as a kind of order parameter for this quantum transition. A diagram is presented as a function of the transparencies of the barriers exhibiting the transport regimes and the transition lines.

I. INTRODUCTION

Interference phenomena and resonance scattering in open quantum chaotic systems have been studied in the last few years with renewed interest since the development of nanoscale devices [1] and breakthrough experiments in quantum dots [2] and microwave billiards [3]. Part of the motivations driving such studies is the intrinsic challenge to find consistent descriptions of quantum mechanical systems coupled to experimentally controllable environments [4,5]. Profound topics such as measurement theory and decoherence phenomena must be considered carefully in the theoretical models and several open questions remain. Consequently, even the theory of noninteracting particles turned out to be quite subtle and is still under development. Fortunately many interesting phenomena can be accommodated in the noninteracting models, as has been evidenced over the years by several experiments in mesoscopic electronic systems.

One of the most attractive features of quantum chaotic scattering is its universal nature. The same stochastic model can be applied to describe phenomena in various physical scales ranging from resonance reactions in atomic nuclei to electron transport in mesoscopic systems and wave propagation in microwave cavities. This provides important fertilizations across boundaries of areas otherwise unconnected. A striking example is the optical model of nuclear reactions [6], which describes the complex scattering characteristics of a resonance reaction in terms of two well separated time scales: an immediate response associated with direct fast processes and a delayed response corresponding to the formation and decay of long-living states (the compound nucleus). This optical model was further developed by Mahaux and Weidenmüller [7] into a powerful scattering-matrix approach to nuclear reactions and culminated with the case study exact calculation, by Verbaarschot, Weidenmüller, and Zirnbauer (VWZ) [8], of the correlation function of the S matrix at different energies using random matrix theory and the supersymmetry method. In this approach, universality appears as a consequence of the requirement that the number of resonances in a relevant energy range (away from thresholds) is much larger than the number of open scattering channels. Quite remarkably, the VWZ model provides one of the most successful descriptions of generic chaotic quantum scattering in the ergodic regime.

The universality observed in the statistical properties of the resonance part of the scattering matrix strongly suggests the possibility of an alternative approach, in which the full distribution function of S-matrix elements is derived from generic principles, without any reference to the underlying Hamiltonian. This program was implemented by Mello and co-workers [9], who demonstrated that under very mild assumptions of minimum information, causality, analyticity, and symmetry constraints the S-matrix distribution function turns out to be proportional to the Poisson kernel. This function leads to a high-dimensional generalization of the Poisson integral formula that appears in the classical two-dimensional electrostatic problem of determining the potential inside a bounded circular domain from the value it takes on the surface. The generalized multidimensional Poisson's integral formula covers a Shilov boundary [10] (a minimal subset of topological boundaries) so that any analytical function inside the bounded domain can be determined in terms of the values it takes on the boundary. The kernel of this generalized Poisson's integral is called the Poisson kernel. The equivalence between the VWZ Hamiltonian approach and Mello's S-matrix approach was established in Refs. [11,12].

A particularly striking effect in open quantum systems is the resonance trapping phenomenon [4,5]. As the coupling strength to continua increases resonances start to overlap and the levels interact strongly in the complex plane exhibiting avoided crossings. At a critical value of the coupling a reor-

ganization of the entire spectrum takes place creating a bifurcation in the lifetimes of the resonance states. Some states align with the decay channels and become very unstable, whereas the rest of the resonances approach the real axis and become long lived. An experimental observation of this phenomenon in a microwave billiard has recently been reported [3]. The generic dynamical principle underlying the whole process is a kind of self-organization associated with a reduction in the number of relevant states and a consequent increase in the system's stability [4]. Rather interestingly, under certain conditions it can be shown [13] that this redistribution of the resonances satisfy the requirements of a second order phase transition.

An important question addressed by Lehmann, Saher, Sokolov, and Sommers [14] is the effect on the statistical properties of S-matrix elements of the above described resonance spectrum reorganization. The importance of this point can be appreciated through the observation that the VWZ approach predicts universal expressions for correlations of S-matrix elements, on a small energy domain about the center of the spectrum ($E=0$), in terms of certain transmission coefficients, $0 \leqslant T_n \leqslant 1$, interpreted as a measure of the part of the incident flux in channel n that penetrates the interacting region and participates in the formation of the long-living states. The coupling of the internal states to the scattering continua is measured by a parameter, $0 < w_n < \infty$, related to T_n through the formula $T_n = 4 w_n / (1 + w_n)^2$. The reordering of the resonance spectrum takes place when some coupling constants exceed the critical value $w_n = 1$. By further increasing these coupling parameters, so that $w_n \geqslant 1$, broad resonances are formed and move away from the real axis, as demonstrated in Ref. [14] through a numerical plot of clouds of S-matrix poles. The key observation is the fact that T_n is invariant under the transformation $w_n \rightarrow 1/w_n$ and consequently the universal fluctuation properties of S-matrix elements are insensitive to this transition. The authors of Ref. [14] proved that by relaxing the VWZ requirement, the number of resonances being much larger than the number of open scattering channels, one can construct nonuniversal models in which the resonance trapping transition affects the correlation functions of S-matrix elements. Although the resonance trapping phenomenon itself does not affect the stochastic properties of the S-matrix characteristics in the universal regime, the underlying mechanism (avoided crossings in the resonance-pole plane) imparts notable features onto transport observables of two-terminal systems, as we shall demonstrate in this work using random-matrix theory.

The successful application of random matrix models to quantum transport led to the development of important theoretical tools to describe resonance scattering through multiterminal chaotic systems [15]. A particularly useful concept for systems attached to two waveguides (or leads) is the density of transmission eigenvalues τ_j, i.e., eigenvalues of $tt^\dagger$, where t is the transmission matrix. This density, defined as $\rho(\tau) = \sum_j \langle \delta(\tau - \tau_j) \rangle$, encompasses all statistical information necessary to compute the average value of several transport observables, such as conductance, shot-noise power, or an arbitrary moment of the charge-counting statistics. In the semiclassical limit, defined by a large number of open scattering channels, transport observables acquire a very narrow

Gaussian distribution and the average value obtained from $\rho(\tau)$ contains all statistically relevant information about the observable. In this semiclassical limit, $\rho(\tau)$ exhibits a rather interesting feature: an inverse square-root singularity at $\tau = 1$ whenever Fabry-Perot resonances are formed between the two barriers at the leads-sample interfaces. This property has proved to be rather robust and was observed in a variety of disordered conductors and ballistic chaotic cavities. In fact, Nazarov and Kindermann [16] claimed that its presence or absence might be used as an indicator for the existence of two broad universality classes in quantum transport. Clearly, the density of transmission eigenvalues is an important probe to the effects of avoided crossings of resonance poles in the universal transport regime and a detailed study of this problem is the main motivation of this paper.

In this work, we consider an open quantum system consisting of a chaotic ballistic cavity coupled, via barriers of arbitrary transparencies, to two semi-infinite waveguides. We describe the ergodic dynamics of the system using two approaches: A numerical implementation of the VWZ model in the semiclassical limit and analytical calculations by means of a recent extension, proposed in Ref. [17], of Nazarov's circuit theory [18]. We show that Fabry-Perot modes, identified as an inverse square-root singularity in $\rho(\tau)$, can be used as a kind of order parameter for a quantum transition, driven by varying the relative strength of the transparencies of the barriers. We present a diagram exhibiting various transport regimes in the system. In Sec. II, we present the stochastic model used to describe the ergodic dynamics inside the chaotic cavity, the scattering matrix, and its resonance poles and the coupling parameters with the associated time scales. In Sec. III, we present in detail the technical aspects of the formalism used to calculate the asymptotic of the Poisson kernel. It has the form of an extended version of Nazarov's two-terminal circuit theory. Several examples are worked out to illustrate the usefulness of the approach. The quantum transition is presented in Sec. IV as an advanced application of circuit theory and is compared with a direct numerical simulation of the Poisson kernel. A continuum Coulomb gas model is used to characterize the various transport regimes that are displayed in the diagram. A summary and conclusions are presented in Sec. V.

II. STOCHASTIC MODEL

In this section we give a brief presentation of the stochastic model used in this work. Although all numerical routines used in this paper are entirely based on this model, we provide here only enough detail to make the interpretations of the results presented in subsequent sections self-contained. Additional information can be found in the cited references and in Appendixes A and B. In Appendix A, we introduce the resonance pole complex plane, which is the arena where level interactions take place, and partial decay width amplitudes, which are parameters that control the strength of the coupling to the leads thereby affecting all transport observables. The combined effect of them is responsible for the onset of the transition addressed in this paper. In Appendix B we present an important discussion about the relevant time scales in the problem.

In the VWZ approach a central quantity is the S-matrix formula below, that describes the coupling of the states in the cavity with a continua of asymptotic free scattering states in waveguides,

$$S(E) = 1 - 2\pi i W^\dagger G^r(E) W, \tag{1}$$

in which $G^r(E)$ is the retarded Green's function defined as

$$G^r(E) = (E - H_{cav} - \Sigma^r)^{-1}. \tag{2}$$

The Hamiltonian of the cavity, H_{cav}, is described by an $N_{cav} \times N_{cav}$ random Hermitian matrix with real entries and

$$\Sigma^r = -i\pi W W^\dagger = -i\pi \sum_{p=1}^M W_p W_p^\dagger \tag{3}$$

is the self-energy function associated with particle exchange between the cavity and M waveguides (terminals). The coupling matrix W is a nonrandom $N_{cav} \times N_{tot}$ rectangular matrix, where $N_{tot} = N_1 + \cdots + N_M$ is the total number of open channels (N_p is the number of open channels in terminal p). We assume absence of direct (nonresonant) reactions by imposing the orthogonality relation

$$(W_p^\dagger W_q)_{nm} = \frac{\lambda}{\pi} \delta_{pq} \delta_{nm} w_{pn}, \tag{4}$$

where $w_{pn} \geq 0$ quantifies the coupling strength of resonance states in the cavity with the scattering channel n in terminal p and $L = 4\lambda$ is the total length of the spectrum (bandwidth).

The random Hamiltonian models the chaotic ergodic motion inside the cavity and is considered to be a member from the Gaussian orthogonal ensemble (GOE), which is appropriate to describe systems with time-reversal symmetry. We thus have the following basic ensemble averages:

$$\langle (H_{cav})_{\mu\nu} \rangle = 0, \tag{5}$$

and

$$\langle (H_{cav})_{\mu\nu} (H_{cav})_{\mu'\nu'} \rangle = \frac{\lambda^2}{N_{cav}} (\delta_{\mu\mu'} \delta_{\nu\nu'} + \delta_{\mu\nu'} \delta_{\nu\mu'}), \tag{6}$$

which, in turn, yield the following asymptotic ($N_{cav} \gg 1$) expression for the average retarded Green's function:

$$\langle G^r(E) \rangle = \frac{\xi(E)}{\lambda} [1 - \lambda^{-1} \xi(E) \Sigma^r]^{-1}, \tag{7}$$

where

$$\xi(E) = \eta(E) - i\zeta(E) = \frac{E}{2\lambda} - i\sqrt{1 - \left(\frac{E}{2\lambda}\right)^2}. \tag{8}$$

From Eq. (7) we obtain a semicircle distribution for the resonance energies (real part of the resonance poles),

$$\sigma(E) = -\frac{1}{\pi} \text{Im} \langle \text{Tr}[G^r(E)] \rangle = \frac{N_{cav}}{\pi\lambda} \zeta(E). \tag{9}$$

The meaning of the ensemble averages above is somewhat subtle. In order to appreciate it one should bear in mind that the stochastic approach models the universal *local in spectrum* features of realistic chaotic systems. This means that if

one wishes to compare the predictions of the stochastic model with raw data one should perform a *local* energy average inside an interval that is sufficiently large to contain many resonances but small enough so that the gross features of the spectrum, such as the mean spacing of resonances, does not vary appreciably. In this sense, global features such the semicircle law should not be considered as valid predictions of the stochastic model, albeit it may be consistently used in intermediate calculations to obtain local in spectrum properties.

Combining Eq. (7) with Eq. (1) we obtain an ensemble average description of the optical (smooth) part of the scattering matrix. In this time scale, the fraction of the incoming flux that enters the cavity from channel n through terminal p can be quantified by the following transmission coefficient associated with an effective barrier at the cavity-waveguide interface,

$$T_{pn}(E) \equiv 1 - |\langle S_{nn}^{pp}(E) \rangle|^2. \tag{10}$$

From Eq. (7) we obtain

$$\langle S_{nm}^{pq}(E) \rangle = \delta_{pq} \delta_{nm} \frac{1 - i w_{pn} \xi(E)}{1 + i w_{pn} \xi(E)} \tag{11}$$

and therefore

$$T_{pn}(E) = \frac{2\zeta(E)}{\kappa_{pn} + \zeta(E)}, \tag{12}$$

where $\kappa_{pn} = \cosh \alpha_{pn}$ and $\alpha_{pn} = -\ln w_{pn}$.

III. ASYMPTOTICS OF THE POISSON KERNEL AND CIRCUIT THEORY

In this section we present in detail our main analytical tool, which is basically an extended version of the two-terminal case of Nazarov's circuit theory [18]. The central different feature of our formalism, in comparison with Nazarov's approach, is the systematization of the subtle process of determining the current-phase relations of the various circuit elements by means of the supersymmetric nonlinear σ model. Our presentation complements a previous short report on this subject [17]. For the benefit of the reader, we have compiled in Appendix C a number of important concepts and results regarding the density of transmission eigenvalues, that are somewhat scattered in the literature and which will be used later to patch up a single unified picture of the mathematical representation of the system. It will also serve the purpose of proving, by sheer comparison with several alternative approaches, the remarkably analytical convenience of our method.

A. Circuit theory for the double-barrier chaotic cavity

The asymptotic limit, $N_1, N_2 \gg 1$, described in Appendix C coincides with the physical semiclassical regime, in which one neglects quantum interference corrections to the particle propagation through the chaotic cavity. A simple consequence of this result is the independence of the asymptotic results on the symmetry parameter β [see Eq. (C8) and the

statement below Eq. (C29)]. This observation opens up the possibility of implementing alternative approaches to determine $\rho(\tau)$. A particularly convenient procedure has the form of a circuit theory and was introduced by Nazarov [18]. It is basically a finite element approach, in which the system is partitioned into a network described by a graph, whose edges represent connectors and the vertices are nodes or terminals. A pseudopotential Φ is assumed to have fixed values at both terminals, $\Phi_1 = \phi$ and $\Phi_2 = 0$, and unknown values at the nodes. Therefore each connector (i,j) is subject to a pseudopotential drop $\Delta\Phi_{ij}$, which generates a pseudocurrent $I_{ij}(\Delta\Phi_{ij})$ defined by

$$I_{ij}(\Delta\Phi_{ij}) = \int_0^1 d\tau \frac{\sin(\Delta\Phi_{ij})\tau\rho_{ij}(\tau)}{1 - \tau\sin^2(\Delta\Phi_{ij}/2)}, \quad (13)$$

where $\rho_{ij}(\tau)$ is the transmission eigenvalue density of the connector. There is a conservation law for the pseudocurrent passing through each node, which provide sufficient equations to determine the value of the pseudopotential at every node.

The problem of determining $\rho(\tau)$ using two-terminal circuit theory proceeds as follows: (i) represent the system as a graph, choosing the connectors to be simple enough so that $I_{ij}(\Delta\Phi_{ij})$ is known; (ii) solve the equations for pseudocurrent conservation and determine the pseudopotential at each node; (iii) determine the current-phase relation $I(\phi)$ for the whole network and using Eq. (C17) derive $\rho(\tau)$. Here we shall need only two circuit elements: a diffusive conductor and a barrier of arbitrary transparency. It is important to note that in circuit theory the current-phase relation of all elements are taken as input, and therefore they must be derived from a microscopic approach, such as the supersymmetric nonlinear σ model (used in this paper) or the more conventional diagrammatic impurity average technique.

In this section, we shall rigorously derive the current-phase relations of the circuit elements and prove the validity of the pseudocurrent conservation formulas to describe the system in the physical regime of interest. Independent numerical evidence of these results will be presented in the next sections. As a model for a chaotic cavity coupled to two waveguides via barriers of arbitrary transparencies we use the supersymmetric nonlinear σ model for an identical system with the cavity replaced by a disordered quasi-one-dimensional conductor of length L and take in the end the limit $L \to 0$. Equation (C12) is then replaced by [19]

$$\Psi_s(Q) = \int dQ' \int dQ'' f_1(Q,Q') W_s(Q',Q'') f_2(Q'',Q_0),$$

$$(14)$$

where $s = 2L/\xi$ and ξ is the localization length. The function $W_s(Q',Q'')$ is the diffusion kernel in $\mathcal{C}$, i.e., it satisfies the diffusion equation

$$(\partial_s - \Delta_Q)W_s(Q,Q') = 0, \quad (15)$$

where Δ_Q is the Laplace-Beltrami operator in the coset space $\mathcal{C} = U(1,1|2)/[U(1|1) \otimes U(1|1)]$, with delta function initial condition

$$W_0(Q,Q') = \delta(Q - Q'). \quad (16)$$

A formal solution is given by following path-integral representation,

$$W_s(Q,Q') = \int \mathcal{D}Q \exp\left(\frac{1}{16s}\int_0^1 dx \text{Str}(\partial_x Q)^2\right), \quad (17)$$

where $\mathcal{D}Q = \Pi_{x=0}^1 dQ(x)$ is the invariant integration measure, Str denotes the supertrace, and we assume the following boundary conditions $Q(0) = Q'$ and $Q(1) = Q$. Note that, as expected, the chaotic cavity corresponds to the zero length limit of the disordered conductor, since $\Psi_0(Q) \equiv \lim_{s\to 0}\Psi_s(Q)$ coincides with $\Psi(Q)$ of Eq. (C12).

This model can be used to determine the current-phase relation of both elements in the circuit theory: the diffusive conductor and the barrier. We start by obtaining the current-phase relation of the diffusive conductor. First we eliminate the effect of the barriers by imposing ideal contacts ($\alpha_{pn} = 0$) and taking $N_1, N_2 \to \infty$, then

$$f_p(Q,Q') \to \delta(Q - Q'), \quad (18)$$

and from Eq. (14) we get $\Psi_s^D(Q) = W_s(Q,Q_0)$. Using the eigenfunctions and eigenvalues of the radial part of the Laplace-Beltrami operator Δ_Q, we may harmonically decompose $\Psi_s^D(Q)$ as follows [19]:

$$\Psi_s^D(Q) = 1 + (\cos\theta_0 - \cosh\theta_1)\sum_{n=0}^{\infty}\int_0^{\infty}d\mu_{nk}$$

$$\times P_n(\cos\theta_0)P_{ik-1/2}(\cosh\theta_1)e^{-\varepsilon_{nk}s}, \quad (19)$$

where $d\mu_{nk} = (\varepsilon_{nk})^{-1}(2n+1)k\tanh(k\pi)dk$ is the integration measure, $\varepsilon_{nk} = k^2 + n(n+1) + 1/4$ is an eigenvalue of the Laplace-Beltrami operator, $P_n(x)$ is the Legendre polynomial, and $P_{ik-1/2}(x)$ is the conical function.

For the pseudocurrent we find from Eqs. (C15) and (19)

$$I_s^D(\phi) = 2\sin\phi\sum_{n=0}^{\infty}\int_0^{\infty}d\mu_{nk}P_n(\cos\phi)P_{ik-1/2}(\cos\phi)e^{-\varepsilon_{nk}s}.$$

$$(20)$$

For $s \ll 1$ we get the following expansion:

$$I_s^D(\phi) = \frac{\phi}{s} - \frac{s}{2}\frac{d}{d\phi}\left[\frac{1}{\phi}\left(\frac{1}{\phi} - \cot\phi\right)\right] + O(s^2). \quad (21)$$

Let us now turn to the current-phase relation of the barriers. We eliminate the contribution of the diffusive conductor by taking $s \to 0$ in Eq. (14). We then isolate barrier 1, by taking the limit $N_2 \to \infty$, which implies $f_2(Q'',Q_0) \to \delta(Q'' - Q_0)$. The integral becomes trivial and yields

$$\Psi^{B1}(Q) = \prod_{n=1}^{N_1}\left(\frac{\cosh\alpha_{1n} + \cos\theta_0}{\cosh\alpha_{1n} + \cosh\theta_1}\right). \quad (22)$$

Using Eq. (C15), we obtain our final answer,

$$I^{B1}(\phi) = \sum_{n=1}^{N_1} \frac{\sin(\phi)T_{1n}}{1 - T_{1n}\sin^2(\phi/2)}. \tag{23}$$

A similar analysis yields the current-phase relation of barrier 2,

$$I^{B2}(\phi) = \sum_{n=1}^{N_2} \frac{\sin(\phi)T_{2n}}{1 - T_{2n}\sin^2(\phi/2)}. \tag{24}$$

We are now in position to implement the equations for pseudocurrent conservation. Our system consists of a diffusive conductor sandwiched between two barriers. The network is a linear graph with two nodes and three connectors, which implies

$$I_s(\phi) = I^{B1}(\phi - \theta_1) = I_s^D(\theta_1 - \theta_2) = I^{B2}(\theta_2), \tag{25}$$

where θ_1 and θ_2 are the values of the pseudopotential Φ, at nodes 1 and 2, respectively. In the semiclassical regime, where $s \ll 1$, we need only to keep the first term in Eq. (21), $I_s^D(\phi) \simeq \phi/s$, and we eliminate θ_1 through $\theta_1 = \theta_2 + sI^{B2}(\theta_2)$, so that $I^{B1}[\phi - \theta_2 - sI^{B2}(\theta_2)] = I^{B2}(\theta_2)$. Define $\theta \equiv \phi - sI^{B2}(\theta_2)$, then

$$I_s(\phi) = \frac{\phi - \theta}{s} = I_0(\theta), \tag{26}$$

where $I_0(\theta)$ is the pseudocurrent through an auxiliary network, in which the diffusive conductor has been removed [17]. The pseudocurrent conservation equations for this auxiliary network is, after obvious renaming of the phase variables, given by

$$I_0(\phi) = I^{B1}(\phi - \theta) = I^{B2}(\theta). \tag{27}$$

From Eq. (26) we get $I_s(\phi) = I_0[\phi - sI_s(\phi)]$, which is the solution of the nonlinear differential equation

$$\frac{\partial I_s}{\partial s} + I_s\frac{\partial I_s}{\partial \phi} = 0, \tag{28}$$

with initial condition $I_{s=0}(\phi) = I_0(\phi)$. This differential equation was derived in Ref. [17] under more general conditions (conductors of arbitrary geometry) and was shown to be equivalent, for quasi-one-dimensional conductors, to the Dorokhov-Mello-Pereyra-Kumar (DMPK) scaling equation [15] for the density of transmission eigenvalues in the semiclassical limit.

In view of our model construction, we conclude that Eqs. (23), (24), and (27) define a circuit theory for a chaotic cavity coupled to waveguides via two barriers of arbitrary transparencies. This is the central result of this section. It represents a formal proof of the concatenation principle used in Ref. [17]. This crucial information was provided by Eq. (14) and by the fundamental notion that the universal statistical description of an open chaotic cavity can be obtained by taking the zero length limit of an identical open system with the cavity replaced by a disordered conductor of finite length. The final conclusion is the realization that circuit theory is an exact representation of the information contained in the saddle point equation of the zero-dimensional supersymmetric nonlinear σ model. A recent striking confir-

mation of this fact can be found in Ref. [20], in which circuit theory equations were shown to agree with the predictions of a diagrammatic analysis of the Poisson kernel in all ranges of the physical parameters.

B. Simple applications of circuit theory

In this section we present further improvements in the formalism of circuit theory and demonstrate its usefulness by working out a few simple examples. We start by introducing a different pseudocurrent through the formula

$$K(x) = \sum_j \left\langle \frac{\sinh 2x}{\cosh 2x + \cosh 2x_j} \right\rangle = \frac{i}{2}I(-2ix), \tag{29}$$

in which the random variables x_j are related to the transmission eigenvalues by $\tau_j = 1/\cosh^2 x_j$. Introducing the average level density $\nu(x) = \sum_j\langle\delta(x-x_j)\rangle$ we may rewrite Eq. (29) as

$$K(x) = \int_0^\infty dy\, \frac{\nu(y)\sinh 2x}{\cosh 2x + \cosh 2y}. \tag{30}$$

This generating function was presented in Ref. [21], where it was used to derive average and variance formulas of linear statistics in the context of the DMPK theory. It can be seen as an integral transform with the kernel

$$\frac{\sinh 2x}{\cosh 2x + \cosh 2y} = \int_0^\infty dk\, \frac{\sin kx \cos ky}{\sinh(k\pi/2)}. \tag{31}$$

Using Eq. (31) we may invert Eq. (30) to obtain

$$\nu(x) = \frac{2}{\pi}\int_0^\infty dk\, \sinh(k\pi/2)\widetilde{K}(k)\cos kx, \tag{32}$$

where

$$\widetilde{K}(k) = \frac{2}{\pi}\int_0^\infty dx K(x)\sin kx, \tag{33}$$

or simply

$$\nu(x) = \frac{2}{\pi}\text{Im}[K(x + i\pi/2 - i0^+)]. \tag{34}$$

The density of transmission eigenvalues $\rho(\tau)$ can be obtained from $\nu(x)$ through the formula

$$\rho(\tau) = \frac{\nu[\cosh^{-1}(1/\sqrt{\tau})]}{2\tau\sqrt{1 - \tau}}. \tag{35}$$

From Eqs. (23), (24), and (30) we obtain the following relation for the pseudocurrent through a barrier with transmission coefficients $T_{pn} = \text{sech}^2(\alpha_{pn}/2)$:

$$K_p(x) = \sum_{n=1}^{N_p} \frac{\sinh 2x}{\cosh 2x + \cosh \alpha_{pn}}. \tag{36}$$

The circuit theory equations for a chaotic cavity sandwiched between two barriers becomes simply

$$K(x) = K_1(x - y) = K_2(y), \qquad (37)$$

where y is the unknown phase variable for the pseudopotential at the intermediate node.

1. Chaotic cavity with ideal contacts

A clean quantum point contact is one of the simplest realization of a chaotic cavity with ideal contacts. In circuit theory we set $T_{pn} = 1 (\alpha_{pn} = 0)$ in Eq. (36) to obtain

$$K_p(x) = N_p \frac{\sinh 2x}{1 + \cosh 2x} = N_p \tanh x, \qquad (38)$$

which when inserted into Eq. (37) yields

$$K(x) = N_1 \tanh(x - y) = N_2 \tanh y. \qquad (39)$$

Using the identity

$$\tanh(x - y) = \frac{\tanh x - \tanh y}{1 - \tanh x \tanh y}, \qquad (40)$$

we obtain the algebraic relation

$$\frac{\eta - \xi}{1 - \xi \eta} = a\xi, \qquad (41)$$

where $\xi = \tanh y$, $\eta = \tanh x$, and $a = N_2/N_1$. Equation (41) implies the quadratic equation

$$a\eta\xi^2 - (1 + a)\xi + \eta = 0, \qquad (42)$$

whose physical solution is

$$\xi_+ = \frac{1 + a}{2a\eta} \left[1 + \sqrt{1 - (\eta\eta_0)^2} \right], \qquad (43)$$

where $\eta_0 = \tanh x_0 = 2\sqrt{a}/(1 + a)$. Inserting Eq. (43) into Eq. (39) yields

$$K(x) = \frac{N_1 + N_2}{2} \coth x \left[1 - \sqrt{1 - \tanh^2 x \tanh^2 x_0} \right]. \qquad (44)$$

Using Eq. (34) we obtain

$$\nu(x) = \frac{N_1 + N_2}{\pi} \sqrt{\tanh^2 x_0 - \tanh^2 x}, \quad 0 < x < x_0, \qquad (45)$$

which after substituting into Eq. (35) yields Eq. (C29) as expected and in agreement with Ref. [18].

2. Chaotic cavity with symmetric barriers

This system can be described in circuit theory by taking $N_1 = N = N_2$ and $T_{pn} = T = \text{sech}^2(\alpha/2)$ in Eq. (36), which gives

$$K_p(x) = N \frac{\sinh 2x}{\cosh 2x + \cosh \alpha}$$

$$= \frac{N}{2} \left[\tanh\left(x + \frac{1}{2}\alpha\right) + \tanh\left(x - \frac{1}{2}\alpha\right) \right]. \qquad (46)$$

Inserting Eq. (46) into Eq. (37) we get the following polynomial equation:

$$(\eta\xi^2 - 2\xi + \eta)[(1 - T)\xi^2 + T\eta\xi - 1] = 0, \qquad (47)$$

where $\xi = \tanh y$ and $\eta = \tanh x$. The physical root is given by

$$\xi_- = \frac{1}{\eta}\left(1 - \sqrt{1 - \eta^2}\right), \qquad (48)$$

which yields the following pseudocurrent:

$$K(x) = \frac{NT \sinh x}{2 - T + T \cosh x} \qquad (49)$$

and average level density

$$\nu(x) = \frac{2N}{\pi} \frac{T(2 - T)\cosh x}{4(1 - T) + T^2 \cosh^2 x}. \qquad (50)$$

Inserting Eq. (50) into Eq. (35) we find

$$\rho(\tau) = \frac{NT(2 - T)}{\pi(T^2 - 4T\tau + 4\tau)\sqrt{\tau(1 - \tau)}}, \qquad (51)$$

which is in precise agreement with Eq. (C30), derived in Ref. [22] from a diagrammatic technique to calculate the asymptotics of the Poisson kernel, for the case of barriers with equivalent channels. We remark that this result cannot be obtained from Nazarov's formulation of circuit theory [18]. One needs the new input provided by the supersymmetric nonlinear σ model, which is incorporated in our extended version in order to establish a direct link with the Poisson kernel.

3. Chaotic cavity with two tunnel junctions

We describe this system in circuit theory by using the condition $N_p = N$ and $T_{pn} = T_p = \text{sech}^2(\alpha_p/2) \ll 1$ in Eq (36). We find

$$K_p(x) = \frac{1}{2} N T_p \sinh 2x. \qquad (52)$$

Substituting Eq. (46) into Eq. (37) we get

$$\sinh(r - s) = \gamma \sinh s, \qquad (53)$$

where $r = 2x, s = 2y$, and $\gamma = T_2/T_1$. The solution reads

$$\sinh s = \frac{\sinh r}{\sqrt{1 + 2\gamma \cosh r + \gamma^2}}, \qquad (54)$$

which, in turn, gives the following expression for the pseudocurrent:

$$K(x) = \frac{NT_1 T_2 \sinh 2x}{2\sqrt{T_1^2 + T_2^2 + 2T_1 T_2 \cosh 2x}}. \qquad (55)$$

For the average level density we find

$$\nu(x) = \frac{2NT_1 T_2}{\pi(T_1 + T_2)} \frac{\sinh x}{\sqrt{\tanh^2 x - \tanh^2 x_0}}, \quad x_0 < x, \qquad (56)$$

where $\tanh x_0 = |T_1 - T_2|/(T_1 + T_2)$. Inserting Eq. (56) into Eq. (35) yields

$$\rho(\tau) = \frac{NT_1 T_2}{\pi(T_1 + T_2)} \frac{1}{\tau^{3/2}\sqrt{\tau_0 - \tau}}, \quad 0 < \tau < \tau_0, \qquad (57)$$

where $\tau_0 = 1 - \tanh^2 x_0 = 4T_1 T_2/(T_1 + T_2)^2$, in agreement with Nazarov's result [18]. The striking difference between Eqs.

(51) and (57) is the absence of the inverse square-root singularity in the latter when $T_1 \neq T_2$. The physical interpretation of this result and some related phenomena will be the subject of the next sections, where it will be associated with a quantum transition.

IV. FORMATION OF FABRY-PEROT RESONANCES AS A QUANTUM TRANSITION

We are now in position to discuss the emergence of the inverse square-root singularity in $\rho(\tau)$ at $\tau = 1$. First, observe from the examples worked out in the previous section that this singularity is regularized by the change of variables, $\tau = \text{sech}^2 x$, so that the new density $\nu(x)$ is finite at $x=0$ if $\rho(\tau)$ has an inverse square-root singularity at $\tau = 1$, and vanishes otherwise. Therefore for symmetric barriers we find

$$\nu(0) = \frac{2NT}{\pi(2-T)} \tag{58}$$

for all values of T, while for tunnel junctions

$$\nu(0) = \begin{cases} NT/\pi; & T_1 = T = T_2 \\ 0; & T_1 \neq T_2. \end{cases} \tag{59}$$

In this section we shall demonstrate that this regularizing property of $\nu(0)$ extends to all values of the ratio T_1/T_2. Therefore it can be used as a kind of order parameter to the quantum transition associated with the emergence of the inverse square-root singularity in $\rho(\tau)$ at $\tau = 1$, which corresponds to the formation of Fabry-Perot (FP) modes between the barriers, implying that $\nu(0)$ could be interpreted as a density of FP resonances. We shall start by considering the simplest case in which the quantum transition occurs, a chaotic cavity with an ideal contact and a barrier of arbitrary transparency, and only later study the most general situation.

A. Chaotic cavity with an ideal contact and a barrier of arbitrary transparency

The description of this system in circuit theory is straightforward and follows the procedure thoroughly explained in last section. We set $T_1 = 1, T_2 = T = \text{sech}^2(\alpha/2)$, and $N_1 = N = N_2$ in Eq. (36) to obtain

$$K_1(x) = N \tanh x \tag{60}$$

and

$$K_2(x) = \frac{N}{2}\left[\tanh\left(x + \frac{1}{2}\alpha\right) + \tanh\left(x - \frac{1}{2}\alpha\right)\right], \tag{61}$$

which after inserting into Eq. (37) yields

$$2\tanh(x-y) = \tanh\left(y + \frac{1}{2}\alpha\right) + \tanh\left(y - \frac{1}{2}\alpha\right). \tag{62}$$

This transcendental equation can be transformed into the following cubic equation:

$$(1-T)\xi^3 + [(2T-1)\tanh x]\xi^2 - (1+T)\xi + \tanh x = 0, \tag{63}$$

where $\xi = \tanh y$.

Before attempting the exact solution let us first construct a solution as a power series in x. Inserting the expansions

$$\xi = ax + bx^2 + cx^3 + \cdots,$$

$$\tanh x = x - \frac{1}{3}x^3 + \cdots$$

into Eq. (63) we obtain $a = 1/(1+T)$, $b=0$, and $c = -[1 + 3T(1-T) + T^3]/[3(1+T)^4]$. This yields the following power series for the pseudocurrent:

$$K(x) = \frac{NTx}{1+T} - \frac{NTx^3(T^3 + 3T - 2)}{3(1+T)^4} + \cdots. \tag{64}$$

This expansion can be used to calculate the average of some transport observables, such as the cumulants of the charge counting statistics. From Eq. (29) we may define the averages

$$h_{k+1} \equiv \sum_j \left\langle \tau_j^{k+1} \right\rangle = \left. \frac{(-1)^k 2^k}{k!} \frac{d^k H(x)}{d(\cosh 2x)^k} \right|_{x=0}, \tag{65}$$

where $H(x) \equiv 2K(x)/\sinh 2x$. From Eqs. (64), (C2), and (65) we obtain the average dimensionless conductance

$$\langle g \rangle = h_1 = \frac{NT}{1+T} \tag{66}$$

and the average shot-noise power

$$\langle p \rangle = h_1 - h_2 = \frac{NT(1+T^2)}{(1+T)^4}. \tag{67}$$

Both expressions are in perfect agreement with Refs. [20,23]. The exact solution for the pseudocurrent reads

$$K(x) = \frac{NT\xi_{sol}}{1 - (1-T)\xi_{sol}^2}, \tag{68}$$

where

$$\xi_{sol} = 2\sqrt{-Q}\cos(\theta/3) - \frac{(2T-1)\tanh x}{3(1-T)}, \tag{69}$$

with $\cos\theta = -R/\sqrt{-Q^3}$, in which

$$Q = \frac{3(T^2-1) - (2T-1)^2\tanh^2 x}{9(1-T)^2} \tag{70}$$

and

$$R = \frac{[9(T-1)(T^2-T+1) - (2T-1)^3\tanh^2 x]\tanh x}{27(1-T)^3}. \tag{71}$$

Let us now turn to the average level density $\nu(x)$. We start by introducing the modified pseudocurrent $\tilde{K}(x) \equiv K(x + i\pi/2)$, then from Eq. (68)

$$\tilde{K}(x) = \frac{NT\tilde{\xi}_{sol}}{1 - (1-T)\tilde{\xi}_{sol}^2}, \tag{72}$$

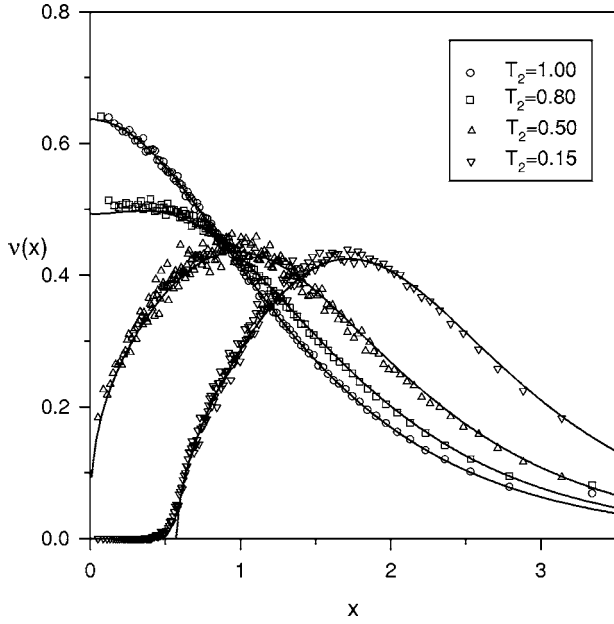where $\tilde{\xi}_{sol}$ is the complex solution of

FIG. 1. Level density $\nu(x)$ for $T_1=1$ and $T_2=1$ (circle), $T_2=0.8$ (square), $T_2=0.5$ (triangle), and $T_2=0.15$ (inverted triangle). The full lines are exact numerical solutions of Eq. (74). Note the transition point at $T_2=0.5$.

$$(1-T)\xi^3 + [(2T-1)\coth x]\xi^2 - (1+T)\xi + \coth x = 0,$$

$$(73)$$

with positive imaginary part, so that

$$\nu(x) = \frac{2}{\pi}\mathrm{Im}[\tilde{K}(x - i0^+)].$$

$$(74)$$

We find

$$\tilde{\xi}_{sol} = -\frac{A+B}{2} - \frac{(2T-1)\coth x}{3(1-T)} + i\frac{\sqrt{3}(A-B)}{2},$$

$$(75)$$

where $A=(R+\sqrt{\Delta})^{1/3}, B=-Q/A$, and $\Delta=Q^3+R^2$. The quantities Q and R are given, respectively, by

$$Q = \frac{3(T^2-1) - (2T-1)^2\coth^2 x}{9(1-T)^2}$$

$$(76)$$

and

$$R = \frac{[9(T-1)(T^2-T+1) - (2T-1)^3\coth^2 x]\coth x}{27(1-T)^3}.$$

$$(77)$$

In Fig. 1, we show the density $\nu(x)$ for several values of the barriers' transparency, T. The symbols (circle, square, triangle, and inverted triangle) correspond to numerical calculations using the Poisson kernel generated from the random Hamiltonian approach described in Sec. II. The numerical procedure is straightforward but quite demanding, since it requires inversion of large $N_{cav} \times N_{cav}$ matrices for each realization. We remark that in order to reach the asymptotic behavior described by $\nu(x)$, one needs a large number, $N_{cav} \gg 1$, of resonances and a large number, $N_{tot} \gg 1$, of open

scattering channels, besides the condition for the emergence of the Poisson kernel, $N_{cav} \gg N_{tot}$, which according to Eq. (B9) implies a large mean delay time, $\bar{Q} \gg 1$.

This explains the noise in the data as a consequence of finite matrix-size effects. Fortunately the numerical implementation of the analytical solution is noiseless and the agreement between both data is excellent. Note that $\nu(0)=0$ for $T \leq 0.5$ and $\nu(0)>0$ for $0.5<T\leq 1$, indicating that $\nu(0)$ plays a role similar to an order parameter in second order phase transitions. Indeed, from the analytical solution, we find

$$\nu(0) = \begin{cases} (2N/\pi)\sqrt{2T-1}; & 0.5 < T < 1 \\ 0; & 0 < T \leq 0.5. \end{cases}$$

$$(78)$$

Another interesting feature of Fig. 1 that can be explicitly extracted from the exact solution is the value of the level, x_0, at which the average density vanishes for $0<T\leq 0.5$, i.e., where $\nu(x_0)=0$. We find

$$x_0 = \tanh^{-1}\left[\sqrt{\frac{(1-2T)^3}{(1-T)(1+T)^3}}\right],$$

$$(79)$$

which agrees quite well with the numerical estimate.

B. Chaotic cavity with two barriers of arbitrary transparencies

This is the most general situation for the case of equivalent channels. In the language of circuit theory, we set $T_p = \mathrm{sech}^2(\alpha_p/2)$ and $N_1=N=N_2$ in Eq. (36) and get

$$K_p(x) = \frac{N}{2}\left[\tanh\left(x + \frac{1}{2}\alpha_p\right) + \tanh\left(x - \frac{1}{2}\alpha_p\right)\right].$$

$$(80)$$

Inserting Eq. (80) into Eq. (37) yields

$$\tanh\left(x - y + \frac{1}{2}\alpha_1\right) + \tanh\left(x - y - \frac{1}{2}\alpha_1\right) = \tanh\left(y + \frac{1}{2}\alpha_2\right)$$
$$+ \tanh\left(y - \frac{1}{2}\alpha_2\right),$$

$$(81)$$

which can be written as the following algebraic equation for the variable $\xi = \tanh y$:

$$[T_1(1-T_2)\tanh x]\xi^4 - (3T_1T_2\tanh x)\xi^2 + [(T_1T_2 + T_2$$
$$- T_1)\tanh^2 x + 2T_1T_2 - T_1 - T_2]\xi^3 + [(T_1T_2 + T_1$$
$$- T_2)\tanh^2 x + T_1 + T_2]\xi - T_1\tanh x = 0.$$

With the physical solution, denoted ξ_{sol}, we can write the exact pseudocurrent as

$$K(x) = \frac{NT_2\xi_{sol}}{1 - (1-T_2)\xi_{sol}^2}.$$

$$(82)$$

From Eqs. (82) and (65) we derive the following expressions for the average conductance and shot-noise power, respectively:

$$\langle g \rangle = N\frac{T_1T_2}{T_1 + T_2},$$
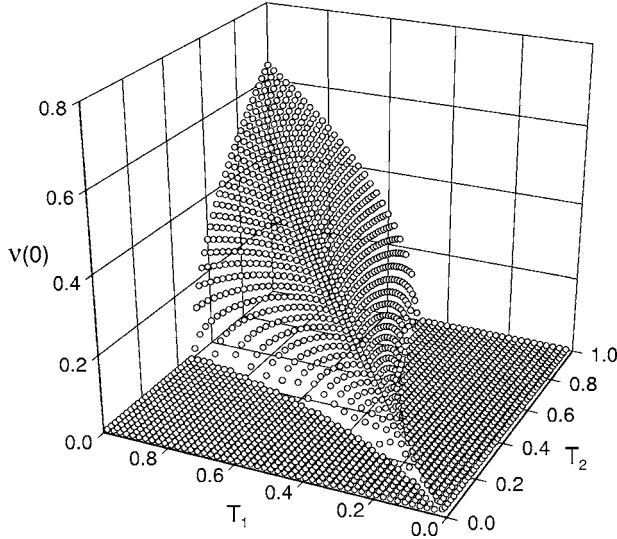
$$(83)$$

and

FIG. 2. Density of Fabry-Perot resonances, $\nu(0)$, as a function of the transmission coefficients T_1 and T_2.

$$\langle p \rangle = N \frac{T_1 T_2 (T_1^2 + T_2^2)}{(T_1 + T_2)^4} (T_1 + T_2 - T_1 T_2). \qquad (84)$$

These formulas are also in agreement with Refs. [20,23]. Consider now the average level density. The modified pseudocurrent is given by

$$\widetilde{K}(x) = \frac{N T_2 \widetilde{\xi}_{sol}}{1 - (1 - T_2) \widetilde{\xi}_{sol}^2}, \qquad (85)$$

where $\widetilde{\xi}_{sol}$ is the physical solution of the following polynomial equation:

$$[T_1(1 - T_2)\tanh x]\xi^4 - (3T_1 T_2 \tanh x)\xi^2 + [(2T_1 T_2 - T_1$$
$$- T_2)\tanh^2 x + T_2 - T_1 + T_1 T_2]\xi^3 + [(T_1 + T_2)\tanh^2 x + T_1$$
$$- T_2 + T_1 T_2]\xi - T_1 \tanh x = 0.$$

It is a simple exercise to verify that all previously considered cases can be obtained directly from the above general equation. The analytical expression of the physical solution $\widetilde{\xi}_{sol}$ is too cumbersome to be reproduced here, but it can be easily generated and manipulated by means of a computer algebra system. In particular, we were able to calculate the following expression:

$$\nu(0) = \frac{2N}{\pi} \text{Re}\left(\frac{\sqrt{(T_1 T_2)^2 - (T_1 - T_2)^2}}{T_1 + T_2 - T_1 T_2} \right). \qquad (86)$$

A three-dimensional plot of $\nu(0)$ is shown in Fig. 2. Note that the support of $\nu(0)$ defines a connected region in the $T_1 T_2$ plane. Interpreting $\nu(0)$ as an order parameter implies that the boundary of this region is given by lines of transition points. To be more precise, consider the new parameters $\zeta_0 = (1 + T_1)/(1 - T_1)$ and $\zeta = T_2(1 + T_1)/T_1$ and rewrite $\nu(0)$ in the form
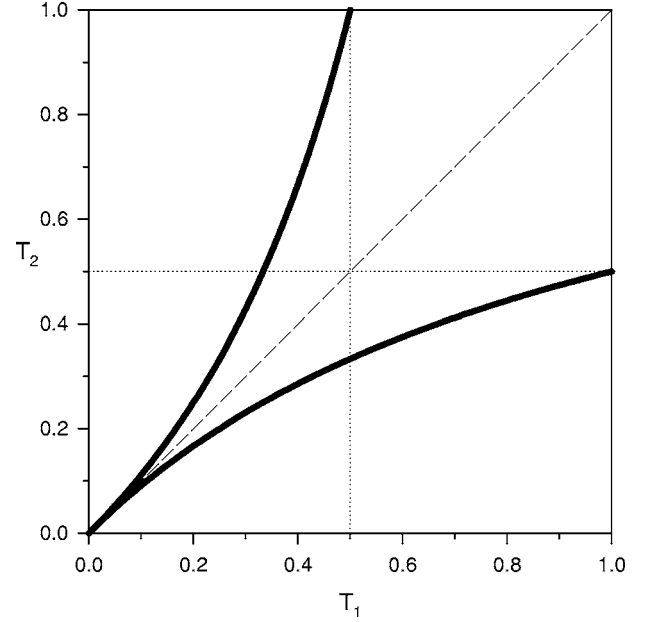

FIG. 3. Diagram illustrating the transport regimes as a function of the tunnel probabilities. The solid lines represent the transition lines $\zeta = \zeta_0$ [case (iv)] and $\zeta = 1$ [case (ii)]. The region above, between and below these solid lines stand for cases (v), (iii), and (i), respectively. The dashed line represents the particular case $T_1 = T_2$, whereas the dotted lines are guides to the eye at $T_1 = 0.5$ and $T_2 = 0.5$.

$$\nu(0) = \frac{2N}{\pi}\begin{cases} \dfrac{\sqrt{\zeta_0(\zeta - 1)(\zeta_0 - \zeta)}}{\zeta + \zeta_0}; & 1 < \zeta < \zeta_0 \\ 0; & \text{otherwise.} \end{cases} \qquad (87)$$

It is now easy to read off the equations $\zeta = 1$ and $\zeta = \zeta_0$ for the boundary lines at which $\nu(0) = 0$. In Fig. 3, we plot a diagram in the $T_1 T_2$ plane exhibiting these transition lines. In the next subsections we shall discuss a characterization of each region in this diagram.

C. Continuum Coulomb gas model

In this subsection we present a simple physical system that can be used to characterize the various regions in the diagram of Fig. 3. It consists of a one-component plasma and is described by the Hamiltonian of a two-dimensional continuum Coulomb gas

$$H = \int d\lambda \mu(\lambda) v(\lambda) + \frac{1}{2} \int d\lambda \int d\lambda' u(\lambda, \lambda') \mu(\lambda) \mu(\lambda'),$$

where $u(\lambda, \lambda') = -\ln|\lambda - \lambda'|$ is the interaction term and $v(\lambda)$ is the effective potential of a compensating background of fixed charge distribution. The equilibrium charge density of this plasma model was discussed in Appendix C and was shown to satisfy the following singular integral equation:

$$\mathcal{P}\int_0^\infty d\lambda' \frac{\mu(\lambda')}{\lambda - \lambda'} = \frac{dv(\lambda)}{d\lambda}. \tag{88}$$

The information contained in Eq. (88) can be nicely accommodated in the resolvent function

$$G(z) = \int_0^\infty d\lambda \frac{\mu(\lambda)}{z - \lambda}, \tag{89}$$

from which the average density and the effective confining potential can be obtained, through the formulas

$$\mu(\lambda) = \frac{1}{\pi}\text{Im}\{G(\lambda - i0^+)\}, \tag{90}$$

and

$$\frac{dv(\lambda)}{d\lambda} = \text{Re}\{G(\lambda - i0^+)\}. \tag{91}$$

It is possible to connect the resolvent function $G(z)$ with the pseudocurrent $K(x)$ of circuit theory by performing the following change of variables: $\lambda = \sinh^2 x$, in Eq. (89), so that

$$G(z) = \int_0^\infty dx \frac{v(x)}{z - \sinh^2 x} = \frac{-K[\cosh^{-1}(\sqrt{-z})]}{\sqrt{z(1 + z)}}. \tag{92}$$

Let us illustrate the usefulness of this formula by considering some simple examples. For a chaotic cavity with symmetric barriers the exact expression for the pseudocurrent is given in Eq. (49), which after inserting into Eq. (92) yields

$$G(z) = \frac{-NT}{\sqrt{-z}[2 + (\sqrt{-z} - 1)T]}. \tag{93}$$

Substituting Eq. (93) into Eqs. (90) and (91) yields, respectively,

$$\mu(\lambda) = \frac{NT(2 - T)}{\pi[(2 - T)^2 + T^2\lambda]\sqrt{\lambda}}, \tag{94}$$

and

$$v(\lambda) = N\ln[(2 - T)^2 + T^2\lambda]. \tag{95}$$

It is interesting to observe the behavior of $G(z)$ for small values of its argument, i.e., $|z| \ll 1$. We find

$$G(z) \simeq -\frac{NT}{2 - T}(-z)^{-1/2} = -\frac{\pi v(0)}{2\sqrt{-z}}, \tag{96}$$

which implies

$$\mu(\lambda) \simeq \frac{NT}{\pi(2 - T)\sqrt{\lambda}} = \frac{v(0)}{2\sqrt{\lambda}}, \quad \lambda \to 0, \tag{97}$$

indicating, since $v(0) > 0$, a gapless transmission spectrum. In order to establish a contrast, consider now the case of tunnel barriers. Inserting Eq. (55) into Eq. (92) we find

$$G(z) = \frac{-NT_1T_2}{\sqrt{(T_1 - T_2)^2 - 4T_1T_2z}}, \tag{98}$$

which, in turn, implies the following average density:

$$\mu(\lambda) = \frac{N(T_1T_2)^{1/2}}{2\pi\sqrt{\lambda - \lambda_0}}, \tag{99}$$

where the nonvanishing value $\lambda_0 = (T_1 - T_2)^2/(4T_1T_2)$ signals the appearance of a gap in the spectrum, i.e., $v(0) = 0$ for $x < x_0 = \sinh^{-1}(\sqrt{\lambda_0})$. In the small argument limit we find a constant,

$$G(z) \simeq -\frac{NT_1T_2}{|T_1 - T_2|}, \quad |z| \to 0. \tag{100}$$

From the examples above, we anticipate the central role played by the resolvent function $G(z)$ in distinguishing the various regimes displayed in the diagram of Fig. 3. A full account of the generic case, with arbitrary T_1 and T_2, is given below.

Consider, for convenience, the variables $\zeta = T_2(1 + T_1)/T_1$ and $\zeta_0 = (1 + T_1)/(1 - T_1)$ and take ζ_0 to be fixed. We identify five different regimes, which we itemize as follows.

(i) $0 < \zeta < 1$ *(gapped phase I).* This regime is characterized by a constant resolvent function in the small argument region,

$$G(z) \simeq \frac{NT_1T_2}{T_1T_2 + T_2 - T_1}, \quad |z| \to 0. \tag{101}$$

The average density has a finite gap, i.e., $v(x) = 0$ for $x < x_0$, where x_0 is a function of both T_1 and T_2.

(ii) $\zeta = 1$ *(transition line I).* In this regime, the resolvent acquires a *universal* power-law behavior,

$$G(z) \simeq -N\left(\frac{T_1^2}{2}\right)^{1/3}(-z)^{-1/3}, \quad |z| \to 0, \tag{102}$$

which implies the following expression for the average density:

$$\mu(\lambda) \simeq \frac{\sqrt{3}N}{2\pi}\left(\frac{T_1^2}{2\lambda}\right)^{1/3}, \quad \lambda \to 0. \tag{103}$$

Accordingly, the average density of transmission eigenvalues develops a power-law singularity,

$$\rho(\tau) \simeq \frac{\sqrt{3}N}{2\pi}\left(\frac{T_1^2}{2(1 - \tau)}\right)^{1/3}, \quad \tau \to 1. \tag{104}$$

The density $v(x)$, on the other hand, vanishes according to the power-law behavior

$$v(x) \simeq \frac{\sqrt{3}N}{\pi}\left(\frac{T_1^2 x}{2}\right)^{1/3}, \quad x \to 0, \tag{105}$$

which is consistent with the corresponding graph displayed in Fig. 1.

(iii) $1 < \zeta < \zeta_0$ *(gapless phase).* In this regime the average level density $v(x)$ is nonvanishing at $x = 0$ and the resolvent function satisfies

$$G(z) \simeq -\frac{\pi v(0)}{2}(-z)^{-1/2}, \quad |z| \to 0, \tag{106}$$

which yields the singularity

$$\mu(\lambda) \simeq \frac{\nu(0)}{2\sqrt{\lambda}}, \quad \lambda \to 0. \tag{107}$$

For the average density of transmission eigenvalues this implies the existence of an inverse square-root singularity at $\tau = 1$,

$$\rho(\tau) \simeq \frac{\nu(0)}{2\sqrt{1-\tau}}, \quad \tau \to 1. \tag{108}$$

The finite value of $\nu(0)$ is given by

$$\nu(0) = \frac{2N}{\pi} \frac{\sqrt{(T_1 T_2)^2 - (T_1 - T_2)^2}}{T_1 + T_2 - T_1 T_2} \tag{109}$$

in agreement with Eq. (86).

(iv) $\zeta = \zeta_0$ *(transition line II)*. This regime is very similar to that of item (ii). The resolvent function satisfies

$$G(z) \simeq -N\left(\frac{T_2^2}{2}\right)^{1/3} (-z)^{-1/3}, \quad |z| \to 0, \tag{110}$$

which implies, as before, the emergence of the universal exponent $1/3$ in all density functions.

(v) $\zeta > \zeta_0$ *(gapped phase II)*. Similar to the gapped phase I, this regime is characterized by a constant resolvent function in the small argument region,

$$G(z) \simeq \frac{N T_1 T_2}{T_1 T_2 + T_1 - T_2}, \quad |z| \to 0, \tag{111}$$

and a finite gap in the average density $\nu(x)$.

D. Physical discussion

From the quantitative analysis of the last subsection we conclude that the formation of Fabry-Perot resonances in a double-barrier chaotic billiard, characterized by the emergence of an inverse square-root singularity in the average density of transmission eigenvalues $\rho(\tau)$ at $\tau = 1$ possesses a number of universal features that strongly resembles second-order phase transitions in statistical mechanics. The average density $\nu(0)$ is nonvanishing only in the gapless phase appearing to be an order parameter and at both transition lines $\zeta = 1$ and $\zeta = \zeta_0$, $\nu(x)$ vanishes according to a power law with a universal exponent. We can make the analogy more striking by defining exponents β, δ, and γ through the relations

$$\nu(0) \sim |t|^{\beta} \tag{112}$$

in the gapless phase,

$$\nu(x) \sim x^{1/\delta} \tag{113}$$

at the transition lines, and

$$G(0) \sim |t|^{-\gamma} \tag{114}$$

in the gapped phases, where $t \equiv \zeta - \zeta_c$, with $\zeta_c = 1$ at transition line I and $\zeta_c = \zeta_0$ at transition line II. From the results of the previous subsection we conclude that $\beta = 1/2, \delta = 3$, and $\gamma = 1$, which satisfy Widom's scaling relation $\gamma = \beta(\delta - 1)$, even though there is no obvious reason for its validity in the

present context. Note that the above values of the exponents coincide with those of classical mean field theory of second order phase transitions. This is a clear consequence of the connection between circuit theory and the saddle-point (mean-field) equation of the zero-dimensional nonlinear σ model in the asymptotic limit of large number of scattering channels, $N_1, N_2 \gg 1$.

A second remarkable analogy follows from the analysis, due to Chalker and Bernhardt [24,25], of the Anderson localization transition, a well known bona-fide second order phase transition. The starting point is the Landauer formula for the dimensionless conductance $g = \sum_{i=1}^N \tau_i$. Consider the change of variables, $\tau_i = \text{sech}^2(L x_i)$, where L is the system's length. The average conductance becomes

$$\langle g \rangle = \int_0^{\infty} dx \frac{2\nu(x)}{\cosh(2Lx) + 1}, \tag{115}$$

where $\nu(x) = \sum_{i=1}^N \langle \delta(x - x_i) \rangle$. We are interested in the scaling limit, $L \to \infty$, with N/L fixed, in which $\nu(x)$ tends towards the density of Lyapunov exponents. In this case we may use the approximation

$$\langle g \rangle \simeq 4 \int_0^{\infty} dx\, e^{-2Lx} \nu(x). \tag{116}$$

In the metallic phase, $\nu(0)$ is nonvanishing and thus from Eq. (116) we find

$$\langle g \rangle \simeq \frac{2\nu(0)}{L} = \frac{N\sigma}{L}, \tag{117}$$

which is Ohm's law and σ denotes the conductivity. In the insulating phase, we have $\nu(0) = 0$ for $x < x_0 = 1/\xi$, where ξ is the localization length, so that

$$\langle g \rangle \sim e^{-2L/\xi}, \tag{118}$$

as expected for an Anderson insulator. At the mobility edge (or transition point) we may try the interpolation ansatz

$$\nu(x) \sim N x^{\alpha}, \tag{119}$$

which yields

$$\langle g \rangle \sim \frac{N}{L^{\alpha+1}} = \frac{L_t^{d-1}}{L^{\alpha+1}}, \tag{120}$$

where L_t is the transverse length of the system. On physical grounds one expects the average conductance to be scale invariant at the mobility edge, i.e., invariant under the transformation, $L \to bL$ and $L_t \to bL_t$, for arbitrary scale factor b. From Eq. (120) we conclude that this is only possible if $\alpha = d - 2$. In summary, we have

$$\nu(x) \begin{cases} \sim \nu(0); & x \to 0 \quad \text{(metallic phase)} \\ \sim x^{d-2}; & x \to 0 \quad \text{(mobility edge)} \\ = 0; & x < 1/\xi \quad \text{(insulating phase)}. \end{cases}$$

For the sake of comparison we also present a summary of the results for the quantum transition studied in this paper

$$\nu(x) \begin{cases} \sim \nu(0); & x \to 0 \quad \text{(gapless phase)} \\ \sim x^{1/3}; & x \to 0 \quad \text{(transition line)} \\ = 0; & x < x_0 \quad \text{(gapped phase)}. \end{cases}$$

The obvious similarities between these results bring additional evidence that our quantum transition might be classified as a kind of second order phase transition. For a complete proof, however, it would be necessary to develop the analog of Landau theory of phase transitions. Since the usual route to derive the Landau expansion, via the physical thermodynamic potential, is not available in our problem, it is not clear, at this moment, how to justify such an expansion for our transition.

Some insight can be gained from a more detailed analysis of the underlying degrees of freedom, which are resonance poles and resonance wave functions. As we have demonstrated, circuit theory provides an exact account of the asymptotic behavior of the average transmission eigenvalue density throughout the whole $T_1 T_2$ diagram. This approach, however, has no access to the underlying mechanism driving the formation of Fabry-Perot modes, which takes place in the resonance pole complex plane, presented in Appendix A. In this language, the problem can be formulated as follows. The transmission eigenvalues, τ_j, can be defined as solutions to the following eigenvalue equation:

$$\sum_m A_{nm} \Psi_m^{(j)} = \tau_j \Psi_n^{(j)}, \tag{121}$$

where A_{nm} is a random Hermitian matrix defined as

$$A_{nm} = \sum_{\mu\nu k} \frac{\gamma_{1n\mu}^r \gamma_{2k\nu}^l (\gamma_{1m\nu}^r \gamma_{2k\mu}^l)^*}{\left(\varepsilon_\mu - \frac{i}{2}\gamma_\mu\right)\left(\varepsilon_\nu + \frac{i}{2}\gamma_\nu\right)} = (A_{mn})^*. \tag{122}$$

The partial decay width amplitudes $\gamma_{pn\mu}^{r,l}$ are random numbers defined in Eq. (A7) and must satisfy the sum rules

$$\sum_\mu \gamma_{pn\mu}^r (\gamma_{pn\mu}^l)^* = 2\lambda w_{pn} \tag{123}$$

and

$$\sum_{pn} |\gamma_{pn\mu}^{r,l}|^2 = \gamma_\mu a_\mu^{r,l}, \tag{124}$$

which establishes a statistical interaction between eigenvectors and eigenvalues in this problem. This correlation could be the reason for the stability of FP states in the case of symmetric barriers. The transmission coefficients of the barriers, T_{pn}, can be connected to the fixed parameters, w_{pn} of Eq. (123), via the relation $T_{pn} = 4w_{pn}/(1 + w_{pn})^2$.

From the analysis of Ref. [14], we know that the resonances form a dense strongly interacting cigar-shaped cloud located below the real axis and stretched alongside it. The precise form of the joint distribution of resonance position is known exactly for systems with broken time-reversal symmetry with an arbitrary number of open channels and resonances [26]. Interestingly, in the limit of large number of open channels it was shown [26] that the n-point correlation function exhibits a Ginibre-like form, i.e., it may be described to a two-dimensional one-component plasma with a

repulsive Coulomb interaction and a nonuniform density. Our problem thus concerns finding the statistical conditions for the appearance of a very large number of transmission eigenvalues close to 1, $\tau_j = 1$, associated with this strongly interacting resonance cloud. Physically, it would explain the formation and stability of FP states between the barriers and answer the question of what competing effects in the resonance plasma can turn their appearance into a phase transition. A similar question was addressed in Ref. [13] in the context of the resonance trapping phenomena. From the form of the random Hermitian matrix A_{nm}, we can see that this problem is quite unconventional, since it involves correlations between both eigenvectors and eigenvalues. We are not aware of any effective analytical method to deal with such problems and numerical simulations appear to be the only way to advance. Solving this open question is one of the challenges that we leave out for future investigations.

Concerning experimental verification of our predictions in noninteracting chaotic billiards, it is important to note that the transition can only affect observables that depend on the overall shape of the average transmission eigenvalue density, such as the characteristic function of charge counting statistics [27]. For weakly interacting quantum dots, it can be shown that the formation of Fabry-Perot resonances leads to the appearance of a different universality class for the low-voltage low-temperature differential conductance (an anomalous power-law I-V characteristic), thus extending the classification put forward in Ref. [16]. Further work in this direction is in progress and will be published elsewhere [28].

V. SUMMARY AND CONCLUSIONS

Quantum scattering through chaotic billiards is a rich and fascinating subject with multiple facets. Its universal features can be successfully described by stochastic models, such as the VWZ approach and random-matrix theory. Depending on the nature of the quantities to be studied, there may be several analytical and numerical techniques to choose from, with varying degrees of mathematical convenience and sophistication. It is often quite hard to connect them in a single unified approach to try and get the best of all worlds. The analytical method presented in this paper has, to some extent, achieved such a unification regarding a particular quantity: the average density of transmission eigenvalues. The method itself can be classified as an extended version of the two-terminal case of Nazarov's circuit theory, but it also combines nicely the saddle-point structure of the supersymmetric nonlinear σ model with the information content of the diagrammatic approach to the asymptotics of the Poisson kernel.

Using this interesting technique, we managed to reduce the calculation of the semiclassical asymptotic form of the average density of transmission eigenvalues, $\rho(\tau)$, to a polynomial equation of forth degree. The resulting expressions include the effects of two barriers of arbitrary transparencies, located at interfaces between the cavity and waveguides. Careful analysis of $\rho(\tau)$ revealed the existence of three different transport regimes, depending on the ratio of the transmission coefficients of the barriers. The rationale of these

regimes could be accommodated in the language of second order phase transitions, with the density of unit transmission eigenvalues playing the role of an order parameter. The associated quantum transition could thus be related to the formation of Fabry-Perot modes between the barriers. A continuum Coulomb gas model was presented as a theoretical tool to interpret this transition as a change in the equilibrium configuration of the plasma due to singular changes in the background density of fixed charges. This procedure led to a characterization of the transition in terms of a resolvent function and certain universal exponents, which were interpreted as having mean field values of an underlying theory of second order phase transition. The dimensional independence of the exponents, typical when critical fluctuations are irrelevant, could be traced back to the ergodic hypothesis adopted to model the chaotic dynamics in the cavity.

We leave as a challenge to future research the derivation of a full-fledged theory of phase transition for the transmission eigenvalue equation in terms of resonance poles and partial decay width amplitudes.

APPENDIX A: RESONANCE POLE COMPLEX PLANE

The most fundamental phenomenon associated with an open quantum system is the decay of an initial population of bound states into a set of scattering channels. In a scattering description, this decay function can be understood in terms of resonance states, characterized by the statistical properties of the S-matrix poles in the complex energy plane. These poles are characterized by both an energy (real part) and a width (twice the imaginary part). In the regime of chaotic scattering these poles are densely packed and exhibit universal interactions, which manifest itself as avoided crossings when the poles acquire a trajectory in the complex energy plane due to the influence of some tunable external parameter. A complete stochastic model for the statistical properties of resonance poles is still not available, although some partial results have proved be to very useful. The subject as a whole, is part of ongoing efforts to develop analytic tools to study weak non-Hermitian random-matrix models [29]. In this appendix, we shall introduce the resonance eigenvalue-eigenvector representation for various quantities of interest. This language will be used later to discuss possible underlying mechanisms of the quantum transition that is the main subject of this paper.

Let $|\Phi_\mu^{r,l}\rangle$ denote, respectively, right and left eigenvectors of the non-Hermitian effective Hamiltonian $H_{eff}=H_{cav}+\Sigma^r$, thus

$$H_{eff}|\Phi_\mu^r\rangle = \left(\varepsilon_\mu - \frac{i}{2}\gamma_\mu\right)|\Phi_\mu^r\rangle, \tag{A1}$$

and

$$\langle\Phi_\mu^l|H_{eff}^\dagger = \left(\varepsilon_\mu - \frac{i}{2}\gamma_\mu\right)\langle\Phi_\mu^l|. \tag{A2}$$

The eigenvectors satisfy the following completeness:

$$1 = \sum_\mu |\Phi_\mu^r\rangle\langle\Phi_\mu^l| = \sum_\mu |\Phi_\mu^l\rangle\langle\Phi_\mu^r| \tag{A3}$$

and biorthogonality relations

$$\langle\Phi_\mu^l|\Phi_\nu^r\rangle = \delta_{\mu\nu}. \tag{A4}$$

Furthermore, one can show that

$$a_\mu^{r,l} \equiv \langle\Phi_\mu^{r,l}|\Phi_\mu^{r,l}\rangle \geqslant 1, \tag{A5}$$

which implies the identity

$$\mathrm{Im}[\langle\Phi_\mu^{r,l}|H_{eff}|\Phi_\mu^{r,l}\rangle] = -\frac{1}{2}\gamma_\mu a_\mu^{r,l}. \tag{A6}$$

We may define new coupling parameters, or partial decay width amplitudes,

$$\gamma_{pn\mu}^{r,l} \equiv \sqrt{2\pi}\langle n|W_p^\dagger|\Phi_\mu^{r,l}\rangle, \tag{A7}$$

in which $|n\rangle$ denotes open-channel states in the pth waveguide. From Eqs. (A6) and (A7) we obtain the following important sum rule:

$$\gamma_\mu a_\mu^{r,l} = \sum_{p=1}^{M}\sum_{n=1}^{N_p} |\gamma_{pn\mu}^{r,l}|^2 = \sum_{p=1}^{M} \langle\Phi_\mu^{r,l}|\Gamma_p|\Phi_\mu^{r,l}\rangle, \tag{A8}$$

where $\Gamma_p \equiv 2\pi W_p W_p^\dagger$.

In this representation the S matrix acquires a rather simple form,

$$S_{nm}^{pq}(E) = \delta_{pq}\delta_{nm} - i\sum_{\mu=1}^{N_{cav}} \frac{\gamma_{pn\mu}^r(\gamma_{qm\mu}^l)^*}{E - \varepsilon_\mu + \frac{i}{2}\gamma_\mu}, \tag{A9}$$

which can be the basis of much insight. When the number of resonances, N_{cav}, tends to infinity with the number of open scattering channels being kept fixed the S-matrix elements $S_{nm}^{pq}(E)$ tend towards a stationary (with respect to energy shifts) universal distribution: the Poisson kernel. This limit is akin to the thermodynamic limit of statistical mechanics and accordingly there is an underlying law of large numbers taking control of the emerging features. This can be nicely formalized in the language of information theory by using a maximum entropy principle.

Likewise, transport coefficients, such as the dimensionless multiterminal conductance $C_{pq}(E)$, defined as

$$C_{pq}(E) \equiv \mathrm{Tr}[\Gamma_p G^r(E)\Gamma_q G^a(E)], \tag{A10}$$

can be written as

$$C_{pq}(E) = \sum_{\mu\nu nm} \frac{\gamma_{pn\mu}^r \gamma_{qm\nu}^l (\gamma_{pn\nu}^r \gamma_{qm\mu}^l)^*}{\left(E - \varepsilon_\mu + \frac{i}{2}\gamma_\mu\right)\left(E - \varepsilon_\nu - \frac{i}{2}\gamma_\nu\right)},$$

$$\tag{A11}$$

and tends towards a universal multivariate stationary distribution as $N_{cav}\to\infty$. Note that the statistical properties of

$C_{pq}(E)$ are determined by both resonance positions and partial decay width amplitudes. Obtaining this distribution is an ongoing challenge for current analytical techniques. The ensemble average $\langle C_{pq}(E) \rangle$ for systems with unitary and orthogonal symmetries was calculated in Refs. [30,31], respectively, using the supersymmetry method. Unitarity of the S matrix implies the following sum rule:

$$\sum_{pq} C_{pq}(E) = \text{Tr}[\Gamma A(E)], \qquad (A12)$$

where $\Gamma = \Sigma_p \Gamma_p$ and $A = i(G^r - G^a) = G^r \Gamma G^a$. In the eigenvalue-eigenvector representation we may write Eq. (A12) as

$$\sum_{pq} C_{pq}(E) = \sum_{\mu} \frac{\gamma_\mu^2}{(E - \varepsilon_\mu)^2 + (\gamma_\mu/2)^2}. \qquad (A13)$$

The ensemble average of Eq. (A13) provides information about the resonance pole density, defined as

$$\sigma(\varepsilon, \gamma) = \sum_{\mu} \langle \delta(\varepsilon - \varepsilon_\mu) \delta(\gamma - \gamma_\mu) \rangle, \qquad (A14)$$

which has been the focus of much attention in the recent literature. We get

$$\sum_{pq} \langle C_{pq}(E) \rangle = \int d\varepsilon \int d\gamma \frac{\sigma(\varepsilon, \gamma) \gamma^2}{(E - \varepsilon)^2 + (\gamma/2)^2}. \qquad (A15)$$

The left hand side of Eq. (A15) can be calculated explicitly using Eq. (7) and yields

$$\sum_{pq} \langle C_{pq}(E) \rangle = \sum_{np} T_{pn}(E)[1 + w_{pn}/\zeta(E)]. \qquad (A16)$$

Combining (A15) and (A16) we obtain an important constraint on $\sigma(\varepsilon, \gamma)$. Another constraint can be derived from the mean delay time [see Eq. (B5)] and reads

$$\bar{Q}(E) = \frac{\hbar}{N_{tot}} \int d\varepsilon \int d\gamma \frac{\sigma(\varepsilon, \gamma) \gamma}{(E - \varepsilon)^2 + (\gamma/2)^2}. \qquad (A17)$$

Of course, a full determination of $\sigma(\varepsilon, \gamma)$ would require an infinite number of such energy dependent constraints. Explicit expressions for $\sigma(\varepsilon, \gamma)$ were derived using a generating function for systems in the absence [32] and presence [33] of time-reversal symmetry.

A particularly useful measure of the system's openness is the total mean width of resonance states, which can be defined from the imaginary part of the effective Hamiltonian, $H_{eff} = H_{cav} + \Sigma^r$, through the formula

$$\bar{\Gamma} = -\frac{2}{N_{cav}} \text{Im}[\text{Tr}(H_{eff})] = \frac{2\lambda}{N_{cav}} \sum_{pn} w_{pn}. \qquad (A18)$$

Defining the mean level distance as $D \equiv L/N_{cav} = 4\lambda/N_{cav}$, we can measure the total coupling strength of the system to the continuum via the ratio

$$\kappa = 2\frac{\bar{\Gamma}}{D} = \sum_{pn} w_{pn}. \qquad (A19)$$

This function can be used to identify various regimes of quantum decay, such as the regimes of overlapping ($\kappa \gg 1$) and isolated ($\kappa \ll 1$) resonances.

In view of possible relevance of reorganizations in the spectrum it is useful to distinguish two types of poles: long-living states (narrow resonances located right below the real axis) and short-living states (broad resonances far away from the real axis). The ensemble average width of long-living states, $\langle \Gamma_l(E) \rangle$, are known to satisfy the Moldauer-Simonius relation [34,35]

$$\prod_{p=1}^{M} \prod_{n=1}^{N_p} |\langle S_{nn}^{pp}(E) \rangle| = \exp[-\pi\sigma(E)\langle \Gamma_l(E) \rangle]. \qquad (A20)$$

Inserting Eq. (11) into Eq. (A20) we find

$$\langle \Gamma_l(E) \rangle = \frac{1}{2\pi\sigma(E)} \sum_{pn} \ln\left(\frac{\kappa_{pn} + \zeta(E)}{\kappa_{pn} - \zeta(E)} \right). \qquad (A21)$$

Following Ref. [32] we define the mean width of long-living states as

$$\bar{\Gamma}_l = \frac{1}{N_{cav}} \int_{-2\lambda}^{2\lambda} dE \sigma(E) \langle \Gamma_l(E) \rangle, \qquad (A22)$$

which yields

$$\bar{\Gamma}_l = \frac{2\lambda}{N_{cav}} \sum_{pn} (\cosh \alpha_{pn} - \sinh|\alpha_{pn}|). \qquad (A23)$$

One can see that if $w_{pn} \leq 1 (\alpha_{pn} \geq 0)$ we obtain $\bar{\Gamma} = \bar{\Gamma}_l$. However, if some subset $(p, n) \in \Omega$ satisfies $w_{pn} > 1 (\alpha_{pn} < 0)$ then a reorganization of the spectrum takes place leading to the appearance of short-lived states strongly coupled to the continuum, thus taking the major portion of the total mean width, so that $\bar{\Gamma} = \bar{\Gamma}_l + \bar{\Gamma}_s$, where

$$\bar{\Gamma}_s = \frac{2\lambda}{N_{cav}} \sum_{(p,n) \in \Omega} \sinh \alpha_{pn} \qquad (A24)$$

is the mean width of the broad resonances. Quite remarkably, in the universal ergodic regime that we consider in this paper, the emergence of this resonance cloud does not yield observable effects in transport observables.

APPENDIX B: TIME SCALES

An important additional source of information about the realization of specific transport regimes in the system is the relative value of certain time scales. For instance, the universal regime we are concerned with is defined by the requirement that the ergodic time t_{erg}, i.e., the time for a wave packet to become uniformly spread throughout the available phase space, be the smallest time scale in the problem. Other time scales are the decay time t_{decay}, which is the time scale for the particle to be emitted from the open cavity, and the

Heisenberg time t_H, which is the time scale for the discrete structure of the spectrum to affect the dynamics.

There are several ways to estimate the above time scales for our cavity problem. A particularly convenient one is via the so-called Wigner-Smith time-delay matrix [36,37] defined as

$$T_{WS}(E) \equiv i\hbar \frac{\partial S^\dagger}{\partial E} S(E). \tag{B1}$$

Consider the ensemble averaged diagonal elements of $T_{WS}(E)$,

$$Q_{pn}(E) = \langle (T_{WS}(E))^{pp}_{nn} \rangle, \tag{B2}$$

and define the mean delay time as

$$\bar{Q}(E) = \frac{1}{N_{tot}} \sum_{pn} Q_{pn}(E) = -\frac{i\hbar}{N_{tot}} \frac{\partial}{\partial E} \langle \ln \det S(E) \rangle. \tag{B3}$$

Using Eq. (1) we get

$$\ln \det S(E) = \mathrm{Tr} \ln \left(\frac{E - H_{cav} - \Sigma^a}{E - H_{cav} - \Sigma^r} \right), \tag{B4}$$

where $\Sigma^a = (\Sigma^r)^\dagger$. Inserting Eq. (B4) into Eq. (B5) we obtain

$$\bar{Q}(E) = -\frac{2\hbar}{N_{tot}} \mathrm{Im}\langle \mathrm{Tr}[G^r(E)]\rangle = \frac{2\pi\hbar\sigma(E)}{N_{tot}}. \tag{B5}$$

The remarkable independence of $\bar{Q}(E)$ on the coupling coefficients was justified in Ref. [11] in terms of the general behavior of the sum of the eigenphases of the scattering matrix upon averaging over an energy interval containing a large number of resonances.

The decay time t_{decay} can be estimated directly from the decay function $P(t)$, i.e., the probability for the compound resonant state to survive until time t if it existed at time $t = 0$. In the limit of strongly overlapping resonances, i.e., a large number of open scattering channels, and near the center of the spectrum $E = 0$, it is given by [4]

$$P(t) = P_0 e^{-\Gamma_{corr} t}, \tag{B6}$$

where

$$\Gamma_{corr} = \frac{\lambda}{2N_{cav}} \sum_{pn} T_{pn} \tag{B7}$$

is the correlation width for fluctuations of S-matrix elements at different energies. In Ref. [14], it was shown that Γ_{corr} coincides with the value of the distance between the uppermost cloud of complex poles of the S matrix and the real energy axis near $E = 0$. This result has a simple interpretation in terms of a stabilization principle [4], according to which for a given degree of overlap between resonances, the system realizes the configuration of resonance positions in complex energy plane, which ensures the slowest decay of the compound. When the coupling to the environment increases beyond a critical value, this is achieved by forming a small cloud of broad resonances that detaches from the initial cloud and by reducing the widths of all other resonances, so that Γ_{corr} reduces thereby increasing the average decay time

of the compound system. A mathematical manifestation of this effect is the invariance of T_{pn} under the transformation $w_{pn} \rightarrow 1/w_{pn}$.

There is an interesting relation between Γ_{corr} and the average of the diagonal elements of the Wigner-Smith time-delay matrix. It reads [4]

$$Q_{pn} = \frac{\hbar T_{pn}}{\Gamma_{corr}}. \tag{B8}$$

The mean delay time near $E = 0$ is then given by

$$\bar{Q} = \frac{1}{N_{tot}} \sum_{pn} Q_{pn} = \frac{2\hbar N_{cav}}{\lambda N_{tot}}, \tag{B9}$$

which coincides with Eq. (B5), since $\sigma(0) = N_{cav}/(\pi\lambda)$.

We shall identify the decay time with the inverse correlation width, so that $t_{decay} \simeq \hbar/\Gamma_{corr}$. A simple estimation of the Heisenberg time is $t_H \simeq \hbar/\Delta$, where $\Delta = 1/\sigma(0) = \pi\lambda/N_{cav}$ is the mean level distance at the center of the spectrum, $E = 0$. The transport regimes of interest can be classified using the dimensionless parameter $g = t_H/t_{decay}$ as follows: (i) the semi-classical regime, where $g \gg 1$, corresponds to the regime of many channels and strongly overlapping resonances ($\Gamma_{corr} \gg \Delta$) (ii) the extreme quantum limit, where $g \simeq 1$, is a regime of few open scattering channels; and (iii) the regime of isolated resonances, where $g \ll 1$ ($\Gamma_{corr} \ll \Delta$). There may be other time scales in the problem associated, for instance, with measurement procedures, but they will not be relevant to our subsequent discussions.

APPENDIX C: TRANSMISSION EIGENVALUE DENSITY AND RELATED CONCEPTS

We shall focus on the two-terminal case, for which the S matrix has the form

$$S = \begin{pmatrix} r & t \\ t' & r' \end{pmatrix} = \begin{pmatrix} S^{11} & S^{12} \\ S^{21} & S^{22} \end{pmatrix}, \tag{C1}$$

where t, t' and r, r' are, respectively, transmission and reflection matrices. The eigenvalues of $tt^\dagger$, denoted τ_j, are called transmission eigenvalues and are the basis of several formulas for transport observables, such as the cumulants of the charge counting statistics, defined as [27,38]

$$q_k = \sum_j \left(\tau(1-\tau) \frac{d}{d\tau} \right)^{k-1} \tau \bigg|_{\tau=\tau_j} \qquad k = 1, 2, \dots. \tag{C2}$$

The first cumulant is simply the dimensionless conductance,

$$q_1 = \sum_j \tau_j = g. \tag{C3}$$

The second cumulant is the dimensionless shot-noise power,

$$q_2 = \sum_j \tau_j (1 - \tau_j) = p. \tag{C4}$$

The third and fourth cumulants have also received much attention and are given, respectively, by

$$q_3 = \sum_j \tau_j (1 - \tau_j)(1 - 2\tau_j) \tag{C5}$$

and

$$q_4 = \sum_j \tau_j (1 - \tau_j)(1 - 6\tau_j + 6\tau_j^2). \tag{C6}$$

More generally, an observable that is a linear statistics of the transmission eigenvalues can be written as

$$A = \sum_j a(\tau_j), \tag{C7}$$

where $a(\tau)$ is an arbitrary function. In the limit of an infinite number of resonances, $N_{cav} \to \infty$, the scattering matrix at the spectrum center $(E=0)$ tends towards the Poisson kernel distribution [9,15]

$$P(S) = C_\beta |\det(1 - S\langle S \rangle^\dagger)|^{-\beta(N_1+N_2-1+2/\beta)}, \tag{C8}$$

where C_β is a normalization constant and

$$\langle S_{nm}^{pq} \rangle = \delta_{pq} \delta_{nm} \tanh(\alpha_{pn}/2). \tag{C9}$$

The parameter β identifies the symmetry class and can assume three values: $\beta=1$ for orthogonal symmetry, $\beta=2$ for unitary symmetry and $\beta=4$ for symplectic symmetry. The Poisson kernel distribution implies that the transmission eigenvalues τ_j's become correlated random variables. Calculation of its correlation functions is a central issue in random matrix theory.

The average of A can be calculated from the average density of transmission eigenvalues, $\rho(\tau) = \Sigma_j \langle \delta(\tau - \tau_j) \rangle$, as

$$\langle A \rangle = \int_0^1 d\tau a(\tau) \rho(\tau). \tag{C10}$$

The information about the barriers at the waveguide-cavity interfaces enters the density $\rho(\tau)$ only through the set of transmission coefficients $T_{pn} = 1 - |\langle S_{nn}^{pp} \rangle|^2$. Apart from its intrinsic practical value indicated above, the density of transmission eigenvalues is also a very useful tool to quantify certain features of resonance interactions in complex energy plane. It will be the central object of our analysis in the body of the paper.

Calculation of $\rho(\tau)$ for arbitrary number of channels and barrier's transparencies has proved to be an exceedingly difficult job [39]. Formally exact expressions, however, can be obtained through the supersymmetry method by means of the generating function introduced by Rejaei [40],

$$Z(\theta_0, \theta_1) = \det\left(\frac{1 - \sin^2(\theta_0/2)tt^\dagger}{1 + \sinh^2(\theta_1/2)tt^\dagger}\right), \tag{C11}$$

where t is the random transmission matrix defined in Eq. (C1). Defining $\Psi(Q)$ as the ensemble average of $Z(\theta_0, \theta_1)$ one can show, e.g., for systems with unitary symmetry ($\beta=2$), that

$$\Psi(Q) = \int dQ' f_1(Q, Q') f_2(Q', Q_0), \tag{C12}$$

in which

$$f_p(Q, Q') = \prod_{n=1}^{N_p} \text{Sdet}^{-1}(1 + e^{-\alpha_{pn}} QQ'), \quad p = 1,2 \tag{C13}$$

describe the coupling of the cavity to the waveguides. The interface's transparencies appear through the variables α_{pn} related to the transmission coefficients T_{pn}, via the identity $T_{pn} = \text{sech}^2(\alpha_{pn}/2)$. We used standard notation for supermathematics: Sdet stands for the superdeterminant and dQ is the invariant measure of the coset space $\mathcal{C} = U(1,1|2)/[U(1|1) \otimes U(1|1)]$. Points in $\mathcal{C}$ are represented by using Efetov's polar coordinates [41],

$$Q = U^{-1} \begin{pmatrix} \cos\hat{\theta} & i\sin\hat{\theta} \\ -i\sin\hat{\theta} & -\cos\hat{\theta} \end{pmatrix} U, \tag{C14}$$

where $\hat{\theta} \equiv \text{diag}(i\theta_1, \theta_0)$, $\theta_1 > 0$, $0 < \theta_0 < \pi$, and U is a supermatrix. The special point, $Q_0 = \text{diag}(1,1,-1,-1)$, represents the origin of $\mathcal{C}$.

In order to make contact with Nazarov's circuit theory, we follow Ref. [17] and define a pseudocurrent as

$$I(\phi) = -2\left(\frac{\partial \Psi}{\partial \theta_0}\right)_{\theta_0 = \phi = i\theta_1} = \sum_j \left\langle \frac{\sin(\phi)\tau_i}{1 - \tau_i \sin^2(\phi/2)} \right\rangle, \tag{C15}$$

in which we used Eq. (C11).

Define the auxiliary function $F(\phi) = I(\phi)/\sin(\phi)$, then

$$F(\phi) = \int_0^1 d\tau \frac{\tau \rho(\tau)}{1 - \tau \sin^2(\phi/2)} = f(\sin^2(\phi/2)), \tag{C16}$$

and therefore

$$\rho(\tau) = -\frac{1}{\pi \tau^2} \text{Im}\left[f\left(\frac{1}{\tau + i0^+}\right) \right]. \tag{C17}$$

Because of the need to evaluate the superdeterminants, Eq. (C12) is too cumbersome for explicit calculations with arbitrary number of channels N_1 and N_2 and thus only particular cases were analyzed in previous works. A particularly favorable situation is that of ideal point contacts, i.e., when $T_{pn} = 1$, in which case calculations simplify considerably and one finds [39]

$$\rho(\tau) = \tau^\alpha \sum_{n=0}^{N-1} (2n + \alpha + 1)[P_n^{(\alpha,0)}(1 - 2\tau)]^2, \tag{C18}$$

where $\alpha = |N_1 - N_2|$, $N = \min(N_1, N_2)$, and $P_n^{(\alpha,\beta)}(x)$ is the Jacobi polynomial. This result is consistent with the following joint distribution of transmission eigenvalues, also known as the Jacobi ensemble [42]:

$$P(\{\tau\}) = C_N \prod_{i<j} |\tau_i - \tau_j|^2 \prod_{i=1}^N \tau_i^\alpha = \frac{1}{N!} \det(K(\tau_i, \tau_j))_{i,j=1,\ldots,N}, \tag{C19}$$

where C_N is a normalization constant and

$$K(\tau,\tau') = (\tau\tau')^{\alpha/2} \sum_{n=0}^{N-1} (2n + \alpha + 1) P_n^{(\alpha,0)}(1 - 2\tau)$$

$$\times P_n^{(\alpha,0)}(1 - 2\tau') \qquad (C20)$$

is a projection kernel with the properties

$$\int d\tau K(\tau,\tau) = N \qquad (C21)$$

and

$$\int d\tau'' K(\tau,\tau'') K(\tau'',\tau') = K(\tau,\tau'). \qquad (C22)$$

The density, Eq. (C18), satisfies $\rho(\tau) = K(\tau,\tau)$. This joint distribution was presented in Ref. [15] and can be derived from random-matrix theory using the maximum information-entropy principle.

It is important to our discussions in Sec. III to understand how the asymptotics, for $N_1, N_2 \gg 1$, of $\rho(\tau)$ can be derived from Eq. (C19). With the change of variables, $\tau_i = 1/(1 + \lambda_i)$, the joint distribution acquires the following Gibbs form:

$$P(\{\lambda\}) = \mathcal{Z}^{-1} \exp(-\beta\mathcal{H}), \qquad (C23)$$

where $\beta = 2$, $\mathcal{Z}$ is the partition function and

$$\mathcal{H} = \sum_i v(\lambda_i) + \sum_{i<j} u(\lambda_i,\lambda_j) \qquad (C24)$$

is the effective Hamiltonian, where $v(\lambda) = (1/2)(N_1 + N_2)\ln(1 + \lambda)$ is a confining potential and $u(\lambda,\lambda') = -\ln|\lambda - \lambda'|$ is a repulsive interaction. Physically, it can be interpreted as a one-component plasma or a logarithmic Coulomb gas with all particles having the same sign of charge. The new level density is defined by $\mu(\lambda) = \sum_{ii}\langle\delta(\lambda - \lambda_i)\rangle$. In the limit $N_1, N_2 \gg 1$ we may use the continuum approximation

$$H = \int d\lambda\mu(\lambda)v(\lambda) + \frac{1}{2}\int d\lambda \int d\lambda' u(\lambda,\lambda')\mu(\lambda)\mu(\lambda').$$

The competition between the confining potential and the repulsive interaction leads to an equilibrium configuration of the levels, which can be obtained from a variational principle, $\delta\mathcal{H} = 0$, subject to the normalization constraint

$$\int d\lambda\mu(\lambda) = N. \qquad (C25)$$

One finds the equilibrium equation

$$v(\lambda) + \int d\lambda' u(\lambda,\lambda')\mu(\lambda') + \text{const} = 0, \qquad (C26)$$

which is equivalent to

$$\mathcal{P}\int_0^\infty d\lambda' \frac{\mu(\lambda')}{\lambda - \lambda'} = \frac{(N_1 + N_2)}{2(1 + \lambda)}. \qquad (C27)$$

The solution to this equation was found by Beenakker [15] and reads

$$\mu(\lambda) = \frac{\sqrt{N_1 N_2}}{\pi(1 + \lambda)}\left(\frac{1}{\lambda} - \frac{1}{\lambda_0}\right)^{1/2}, \qquad (C28)$$

where $\lambda_0 = 4N_1 N_2/(N_1 - N_2)^2$. Switching back to the original variable, $\tau = 1/(1 + \lambda)$, we get

$$\rho(\tau) = \frac{N_1 + N_2}{2\pi\tau}\sqrt{\frac{\tau - \tau_0}{1 - \tau}}, \quad \tau_0 \leq \tau \leq 1, \qquad (C29)$$

where $\tau_0 = 1/(1 + \lambda_0) = [(N_1 - N_2)/(N_1 + N_2)]^2$. As can be seen from the above derivation, this result is independent of $\beta \in \{1, 2, 4\}$ and therefore applies to all symmetry classes.

A similar asymptotic analysis was pursued in Ref. [22] using a diagrammatic method. They managed to treat systems with barriers of arbitrary transparencies. Analytic results for $\rho(\tau)$, however, were only obtained for symmetric barriers, i.e., $T_{1n} = T_{2n} = T_n$ and $N_1 = N_2 = N$. They found

$$\rho(\tau) = \sum_{n=1}^N \frac{T_n(2 - T_n)}{\pi(T_n^2 - 4T_n\tau + 4\tau)\sqrt{\tau(1 - \tau)}}. \qquad (C30)$$

Note that if $T_n = 1$ one gets

$$\rho(\tau) = \frac{N}{\pi}\frac{1}{\sqrt{\tau(1 - \tau)}}, \qquad (C31)$$

in agreement with Eq. (C29) for $N_1 = N_2 = N$. More recently [20] analytical results were obtained for asymmetric barriers and equivalent channels using the same method and complete agreement with circuit theory was found. The singularity at $\tau = 1$, which appears both in Eqs. (C29) and (C30), signals the formation of Fabry-Perot resonance states between the barriers and is the center of our attention in the body of this paper.

[1] For a review, see D. K. Ferry and S. M. Goodnick, *Transport in Nanostructures* (Cambridge University Press, Cambridge, England, 1997).

[2] See, e.g., J. P. Bird *et al.*, Phys. Rev. Lett. **82**, 4691 (1999).

[3] E. Persson, I. Rotter, H.-J. Stöckmann, and M. Barth, Phys. Rev. Lett. **85**, 2478 (2000).

[4] For a review, see F.-M. Dittes, Phys. Rep. **339**, 215 (2000).

[5] J. Okolowicz, M. Ploszajczak, and I. Rotter, Phys. Rep. **374**, 271 (2003).

[6] H. Feshbach, C. E. Porter, and V. F. Weisskopf, Phys. Rev. **96**, 448 (1954).

[7] C. Mahaux and H. A. Weidenmüller, *Shell Model Approach in*

Nuclear Reactions (North-Holland, Amsterdam, 1969).

[8] J. J. M. Verbaarschot, H. A. Weidenmüller, and M. R. Zirnbauer, Phys. Rep. **129**, 367 (1985).

[9] For a review, see P. A. Mello and H. U. Baranger, Waves Random Media **9**, 105 (1999).

[10] S. Helgason, *Geometric Analysis on Symmetric Spaces*, Mathematical Surveys and Monographs No. 39 (American Mathematical Society, Providence, 1994).

[11] C. H. Lewenkopf and H. A. Weidenmüller, Ann. Phys. (N.Y.) **212**, 53 (1991).

[12] P. W. Brouwer, Phys. Rev. B **51**, 16878 (1995).

[13] C. Jung, M. Müller, and I. Rotter, Phys. Rev. E **60**, 114 (1999).

[14] N. Lehmann, D. Saher, V. V. Sokolov, and H.-J. Sommers, Nucl. Phys. A **582**, 223 (1995).

[15] For a review, see C. W. J. Beenakker, Rev. Mod. Phys. **69**, 731 (1997).

[16] M. Kindermann and Yu. V. Nazarov, Phys. Rev. Lett. **91**, 136802 (2003).

[17] A. M. S. Macêdo, Phys. Rev. B **66**, 033306 (2002).

[18] Yu. V. Nazarov, in *Quantum Dynamics of Submicron Structures*, edited by H. Cerdeira, B. Kramer, and G. Schoen (Kluwer, Dordrecht, 1995), p. 687.

[19] A. M. S. Macêdo, Phys. Rev. B **61**, 4453 (2000).

[20] A. L. R. Barbosa and A. M. S. Macêdo, Phys. Rev. B **71**, 235307 (2005).

[21] A. M. S. Macêdo and J. T. Chalker, Phys. Rev. B **49**, 4695 (1994).

[22] P. W. Brouwer and C. W. J. Beenakker, J. Math. Phys. **37**, 4904 (1996).

[23] K. E. Nagaev, P. Samuelsson, and S. Pilgram, Phys. Rev. B **66**, 195318 (2002).

[24] J. T. Chalker and M. Bernhardt, Phys. Rev. Lett. **70**, 982 (1993).

[25] M. Bernhardt and J. T. Chalker (unpublished).

[26] Yan V. Fyodorov and B. A. Khoruzhenko, Phys. Rev. Lett. **83**, 65 (1999).

[27] L. S. Levitov, H. W. Lee, and G. B. Lesovik, J. Math. Phys. **37**, 4845 (1996). For a recent review, see L. S. Levitov, in *Quantum Noise in Mesoscopic Systems*, edited by Yu. V. Nazarov (Kluwer, Dordrecht, 2003).

[28] A. M. S. Macêdo and Andre M. C. Souza (unpublished).

[29] For a recent review, see Yan Fyodorov and H.-J. Sommers, J. Phys. A **36**, 3303 (2003).

[30] A. M. S. Macêdo, Phys. Rev. B **63**, 115309 (2001).

[31] A. M. S. Macêdo, Phys. Rev. B **69**, 155309 (2004).

[32] Yan V. Fyodorov and H.-J. Sommers, J. Math. Phys. **38**, 1918 (1997).

[33] H.-J. Sommers, Yan V. Fyodorov, and M. Titov, J. Phys. A **32**, L77 (1999).

[34] P. A. Moldauer, Phys. Rev. **157**, 907 (1967).

[35] M. Simonius, Phys. Lett. **52B**, 279 (1974).

[36] E. P. Wigner, Phys. Rev. **98**, 145 (1955).

[37] F. Smith, Phys. Rev. **118**, 349 (1960).

[38] D. A. Ivanov, H. W. Lee, and L. S. Levitov, Phys. Rev. B **56**, 6839 (1997).

[39] J. E. F. Araújo and A. M. S. Macêdo, Phys. Rev. B **58**, R13379 (1998).

[40] B. Rejaei, Phys. Rev. B **53**, R13235 (1996).

[41] K. B. Efetov, *Supersymmetry in Disorder and Chaos* (Cambridge University Press, Cambridge, England, 1997).

[42] M. L. Mehta, *Random Matrices* (Academic, New York, 1991).